Bulg. J. Phys. **44** (2017) S81–S92

# Crust-Core Transitions in Neutron Stars Revisited

**X. Viñas**[1], **B.K. Sharma**[2], **C. Gonzalez-Boquera**[1], **M. Centelles**[1]

[1]Departament de Física Quàntica i Astrofísica and Institut de Ciències del Cosmos (ICCUB), Facultat de Física, Universitat de Barcelona, Martí i Franqués 1, E-08028 Barcelona, Spain

[2]Department of Sciences, Amrita School of Engineering, Amrita Vishwa Vidyapeetham, Amrita University, 641112 Coimbatore, India

Received *30 June 2017*

**Abstract.** We have studied the possible existence of pasta phases in the inner crust of neutron stars using the Compressible Liquid Drop Model and the Thomas-Fermi method with Skyrme forces. Special attention is payed to the search of the density corresponding to the crust-core transition. Some properties of this transition, namely density and pressure, are also estimated from the core side using the thermodynamical and dynamical methods. Finally we analyze the impact of the slope of the symmetry energy on the aforementioned properties of the crust-core transition.

PACS codes: 26.60.Gj, 26.60.-c

## 1 Introduction

Neutron stars (NS) are the remnants of massive stars after the supernova explosion [1]. A NS is made of neutrons, protons, leptons and eventually other exotic particles, such hyperons or even quarks, which are distributed in a dense liquid core encompassed by a solid crust. The NS are systems electrically neutral and maintained locally in $\beta$-equilibrium. In the most external part of the star, i.e. in its crust, nucleons are arranged in clusters of positive charge distributed in a solid body centered cubic (bcc) lattice permeated by a gas of free electrons in the outer crust and also by a free neutron gas in the inner crust. The essential input for computing most of the properties of NS is the Equation of State (EOS) of neutron-rich matter. In the outer crust the EOS is essentially determined by the nuclear masses [2], which are experimentally known up to average densities of $4 \times 10^{11}$ g/cm$^3$. From this density on, masses are provided by successful mean field models, in both relativistic and non-relativistic frames [3–6]. In the inner crust, the fraction of free neutrons grows when the matter density

increases up to a density about one half of the nuclear matter saturation density. At this density the transition to the core occurs because it is energetically favourable for the system to change from the solid to a liquid phase. At the deepest layers of the inner crust the nuclear clusters may adopt shapes different from the spherical one, i.e. the so-called "pasta phases", in order to minimize the Coulomb energy. A full quantal treatment of the inner crust is a very complicated task owing to the presence of the neutron gas as well as the eventual need to describe non-spherical structures. From the seminal paper of Negele and Vautherin [7], the Wigner-Seitz approach (WS) has been widely used in calculations of the inner crust at mean field level. In this approach the inner crust is modelized by a set of non-interacting WS cells, each one containing a single nuclear cluster plus the corresponding electron and neutron gases. In this way it is possible to describe the whole crust, assumed to be composed by spherical nuclei only, at Hartree-Fock level including pairing correlations [8–11]. Due to the fact that the inner crust is largely dominated by the neutron gas and shell effects are to certain extent marginal, semiclassical approaches, which do not include shell effects, are very useful to describe the inner crust of NS including non-spherical shapes. The simplest approach is the so-called Compressible Liquid Drop Model (CLDM), which was devised by Baym, Bethe and Pethick [2] as an extension of the mass formula but taking into account explicitly the gases of electrons and dripped neutrons. The CLDM approach has been used in some unified EOS, which describe the crust and the core with the same effective interaction [12, 13]. A more elaborated treatment of the inner crust is provided by the Thomas-Fermi (TF) approximation, which takes into account the different contributions to the energy, i.e bulk, surface and Coulomb, in a self-consistent manner. Calculations of TF type, including pasta phases, have been carried out in the non-relativistic [6, 14–16] as well as in the relativistic [17–20] frames. More involved treatments of the inner crust are available nowadays in the literature. These advanced descriptions of the inner crust include Hartree-Fock calculations in cubic cells and also calculations beyond the WS approximation (see [6] for more references).

Let us now consider the core of the NS. Due to the fact that we are mainly interested in analyzing the transition from the core to the crust, we restrict ourselves to consider NS cores composed by neutrons plus a fraction of protons and electrons, which maintain the system charge neutral and in $\beta$-equilibrium. The structure of the core is much simpler that the one of the crust because the distribution of the different particles is uniform. This allows to describe the core by means of sophisticated *ab initio* calculations, as for example the ones used in the unified microscopically based BCPM EOS [6]. In this work we will use effective interactions of Skyrme type by two reasons. On the one hand, we want to compare our estimates of the crust-core transition densities computed from the core side with the predictions obtained from the crust side with the CLDM and the TF approximation using the same Skyrme force. On the other hand, we

want to investigate possible correlations between some properties of the crust-core transition with the slope of the symmetry energy $L$. To this end, one needs a relatively large set of nuclear models covering a wide range of $L$, which is provided by the Skyrme forces. In order to estimate the crust-core transition it is simpler to go from the core to the crust instead of going from the crust to the core, as we have briefly discussed in [21]. Proceeding from the core side, the search of the crust-core transition density is reduced to find the density for which the uniform system becomes unstable against the formation of nuclear clusters.

The paper is organized as follows. In Secs. 2 and 3 we review the CLDM and TF methods used to describe the inner crust including pasta phases and paying special attention in determining the crust-core density transition from the crust side. Sec. 4 is devoted to study the crust-core transition from the core side, analyzing possible correlations between crust-core transition properties and the slope of the symmetry energy. Our conclusions are given in the last section.

## 2 The Compressible Liquid Drop Model (CLDM) for the Inner Crust of Neutron Stars

The Compressible Liquid Drop Model (CLDM) is a popular approach to describe the inner crust of NS [2, 22] (see also [13] and references therein). In the CLDM one can separate the bulk, surface and Coulomb contributions to the total energy density $\mathcal{E}_{cell}$ within the WS cell. The nuclear structures are arranged as a dense nuclear cluster, which fills a fraction $\chi$ of the total volume of the cell $V_c$, a less dense free neutron gas in the remaining volume of the cell and electrons, which fill the whole cell and are described as a relativistic uniform Fermi gas.

Thus the total energy density $\mathcal{E}_{cell}$ is given by

$$\mathcal{E}_{cell} = \mathcal{E}_{bulk} + \mathcal{E}_{surf} + \mathcal{E}_{Coul} + \mathcal{E}_{elec}, \tag{1}$$

where $\mathcal{E}_{bulk}$, $\mathcal{E}_{surf}$, $\mathcal{E}_{Coul}$ and $\mathcal{E}_{elec}$ are the contributions to the energy density from the bulk, surface, Coulomb and electrons, respectively. The bulk contribution does not depend on the shape of nuclear structures, while the surface and Coulomb do it. The free neutron gas has two main effects on nuclear clusters: first, it reduces the surface tension $\sigma_{surf}$ and, consequently, the surface energy of the clusters with increasing density. Second, the neutron gas exerts a pressure on the clusters. In order to describe these two effects consistently, it is important to compute the surface energy effects using a microscopic Hartree-Fock or Extended Thomas Fermi (ETF) approach with the same effective interaction used to obtain the bulk terms [25].

For the different shapes in the inner crust, the nuclear surface is defined by the reference proton radius $R_p$ [25].

Then, the total energy density in the WS cell is given by

$$\mathcal{E}_{cell} = \frac{E}{V_c} = \chi\mathcal{E}\left(n_n, n_p\right) + \left(1-\chi\right)\mathcal{E}\left(n_d, 0\right) + \frac{3\chi\sigma_{surf}}{R_p} + n_{surf}\mu_s + \frac{3}{4}\left(3\pi^2\right)^{1/3}\chi^{4/3}n_p^{4/3} + \frac{4\pi}{5}e^2R_p^2n_p^2\chi\Big(1-\frac{3}{2}\chi^{1/3}+\frac{1}{2}\chi\Big), \quad (2)$$

where $n_n$ and $n_p$ are the neutron and proton densities of the nuclear cluster, $n_d$ is the free neutron gas density and $\mathcal{E}\left(n_n, n_p\right)$ and $\mathcal{E}\left(n_d, 0\right)$ are the corresponding bulk energy densities. With the chosen reference interphase $R_p$ the surface contribution to the total energy in the WS cell consists of the usual surface tension part supplemented by an additional term due to the neutrons adsorbed onto the surface [25]:

$$E_{surf} = \mathcal{A}\sigma_{surf} + N_{surf}\mu_s, \quad (3)$$

where $\mathcal{A}$ is the area of the reference surface, $\sigma_{surf}$ the surface tension, and $N_{surf}$ and $\mu_s$ are the number and the chemical potential of the neutrons adsorbed onto the reference surface. By expanding $\sigma_{surf}$ and $N_{surf}$ around the planar surface up to linear terms in the curvature $\kappa$ [25], one can account for the curvature corrections. For a spherical nucleus ($\kappa = 2/R_p$), one has

$$4\pi R_p^2\sigma_{surf} = 4\pi R_p^2\big[\sigma_s + \frac{2}{R_p}\sigma_c\big], \quad (4)$$

and

$$N_{surf} = 4\pi R_p^2\Big[s_n + \frac{2}{R_p}\frac{b_n^2 - b_p^2 + s_n^2}{2}\Big](n_n - n_d), \quad (5)$$

where $s_n$ is the skin thickness and $b_n$ and $b_p$ the neutron and proton surface widths [23–25]. These quantities as well as the planar surface tension $\sigma_s$ and its curvature correction $\sigma_c$ are obtained through a self-consistent ETF calculation of semi-infinite asymmetric nuclear matter using a nuclear effective interaction [23–25]. The total surface contribution to the energy density in Eq. (2) is given by Eq. (3 divided by the volume of the cell $V_c$.

From a thermodynamical point of view, one shall establish mechanical and chemical equilibrium between the different contributions to $\mathcal{E}_{cell}$ with the constraints of given average baryon density $n_B$ and charge neutrality. The equilibrium conditions are obtained by taking variations respect to the independent variables $n_n$, $n_p$, $n_d$, $n_{surf}$, $\chi$ and $R_p$ [13]. Due to charge neutrality the electron density reads $n_e = \chi n_p$. One obtains

$$\mu_n - \mu_p - \mu_e = \frac{8\pi}{5}e^2R_p^2n_p\Big(1-\frac{3}{2}\chi^{1/3}+\frac{1}{2}\chi\Big) \quad (6)$$

$$P_i - P_o = \frac{2}{R_p}\Big(\sigma_s + \frac{\sigma_c}{R_p}\Big) - \frac{4\pi}{15}e^2R_p^2n_p^2(1-\chi) \quad (7)$$

$$4\pi R_p^2\Big(\sigma_s + \frac{4\sigma_c}{R_p}\Big) = \frac{32\pi^2}{15}e^2R_p^5n_p^2\Big(1-\frac{3}{2}\chi^{1/3}+\frac{1}{2}\chi\Big), \quad (8)$$

where $\mu_n = \partial\mathcal{E}\left(n_n, n_p\right)/\partial n_n$, $\mu_p = \partial\mathcal{E}\left(n_n, n_p\right)/\partial n_p$ and $\mu_e = \partial\mathcal{E}_{elec}\left(n_e\right)/\partial n_e$ are the neutron, proton and electron chemical potentials. Eq. (6) and (7) correspond to the $\beta$-equilibrium and pressure-equilibrium conditions for the inner crust, respectively. Eq. (8), which can be recast as $E_{surf} + 2E_{cur} = 2E_{coul}$, is known as the virial theorem. The total pressure can be written as $P = P_o + P_L + P_e$, where $P_o$ is pressure from free neutron gas, while $P_L = -\partial E_{coul}/\partial V_c$ and $P_e$ are the lattice and electron pressure contributions. Similarly, we have obtained the equations for the other shapes i.e., rod, slab, tube and bubble respectively (see [21] for further details).

In Figure 1, we plot the energy densities for different shapes of the WS cells computed with the CLDM using the Skyrme interactions SLy4 and SkX. For each force we substract the bulk value to the energy density corresponding to each shape because the bulk part is the same for a fixed average density $n_B$. We find that the rod shape is close in energy to the sphere (nuclei) and the difference

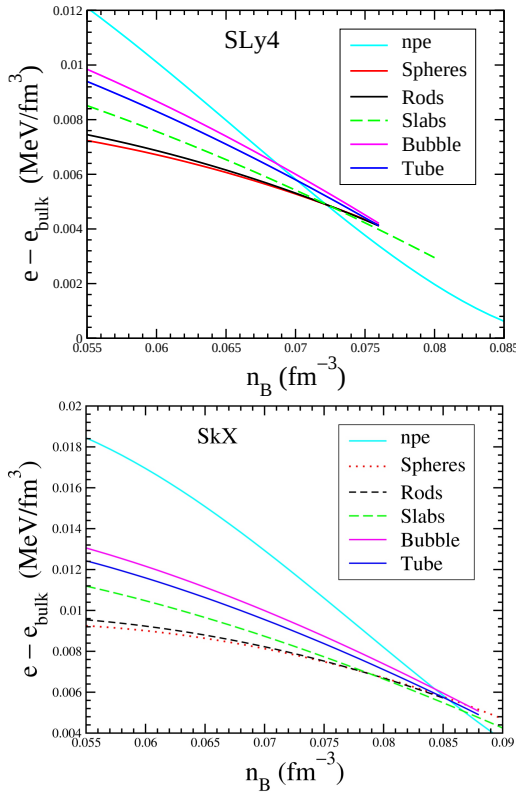


Figure 1. CLDM energy density of different shapes of the WS cells minus the bulk contribution as a function of the average density $n_B$ for the SLy4 and SkX Skyrme interactions.

decreases with increasing $n_B$. For these forces, the spheres (nuclei) is the most favorable structure up to densities around 0.075 fm$^{-3}$, where non-spherical geometries become the preferred shapes, which indicates the appearance of pasta phases. SLy4 reaches the crust-core transition at a lower density of 0.072 fm$^{-3}$ and, therefore, it does not predict nuclear pasta in the inner crust. Nuclear pasta appears in the case of the SkX force, whose transition density of 0.086 fm$^{-3}$ is high enough to allow non-spherical shapes as the most stable configurations.

## 3 Thomas-Fermi Model for the Inner Crust of Neutron Stars

Another relatively simplified model to describe the inner crust of NS is the TF method, which is a semiclassical treatment of the many body system. The basic idea behind the TF method is that if the quantum numbers which describe the many body system vary continuously, one can use the number densities of the various constituent particles of the system instead of their wave functions. This approximation is valid when the characteristic length scales of the density variations are much larger than the corresponding interparticle spacings. The TF approach can be improved by including the gradients expansion of the kinetic energy part of the energy density functional (ETF) [26]. We know that the inner crust is largely dominated by the free neutron gas and that shell effects and pairing correlations play a minor role. This supports that the TF treatment of the EOS in the inner crust be a reliable approximation in this region of the NS. Also, as far as shell effects are neglected in the TF method, it is well suited for dealing with non-spherical shapes of the WS cells.

The total energy density of the inner crust in the TF approach is given by

$$\mathcal{E} = \mathcal{H}\left(n_n, n_p\right) + \mathcal{E}_{elec} + \mathcal{E}_{Coul} + \mathcal{E}_{ex} + m_n n_n + m_p n_p, \tag{9}$$

where $\mathcal{H}$, $\mathcal{E}_{elec}$, $\mathcal{E}_{Coul}$, and $\mathcal{E}_{ex}$ are the nuclear, electron, Coulomb direct and exchange contributions to the total energy density, respectively. In the TF approach, $\mathcal{H}$ is given by

$$\begin{aligned}\mathcal{H}\left(n_n, n_p\right) = &\frac{\hbar^2}{2m_n}\frac{3}{5}\left(3\pi^2\right)^{2/3} n_n^{5/3}(\vec{r}) \\ &+ \frac{\hbar^2}{2m_p}\frac{3}{5}\left(3\pi^2\right)^{2/3} n_p^{5/3}(\vec{r}) + \mathcal{V}\left(n_n(\vec{r}), n_p(\vec{r})\right), \end{aligned} \tag{10}$$

where the first terms are the neutron and proton TF kinetic energy densities and $\mathcal{V}\left(n_n, n_p\right)$ is the interacting part produced by the considered effective interaction. From Eq. (9) one can derive the variational equations obeyed by the particle densities for a WS cell satisfying $\beta$-equilibrium and charge neutrality. More details about the TF approach to the inner crust and the solution of the associated variational equations can be found in previous works [6, 21, 27]. The same TF method used for spherical WS cells can be easily extended to deal with other

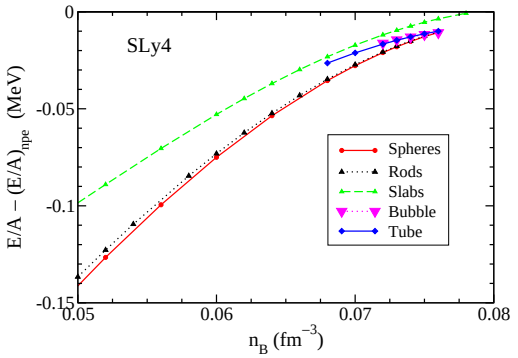


Figure 2. TF energy per baryon of different shapes relative to uniform $npe$ matter computed with the SLy4 force as a function of the baryon density in the inner crust.

geometries, such as rods and slabs [6, 21]. In the TF method the bulk, surface and Coulomb contributions are coupled among them, instead of being treated as separated pieces as it happens in the case of the CLDM discussed in the previous section. The self-consistent TF method has been applied recently to obtain the EOS of the inner crust of NS in Ref. [6, 21, 28] using the so-called BCPM energy density functional [29, 30]. Here we present our TF study of the inner crust using the SLy4 interaction, which is a Skyrme-type force developed with a focus on neutron-rich nuclei and the equation of state of neutron matter [31].

In Figure 2 we display the TF energy per baryon minus the energy per particle in uniform *npe* matter as a function of the average density $n_B$ of the WS cell. As we can see, the predictions for the energetic ordering of the different pasta shapes obtained in the previous section with the CLDM are in good agreement with those obtained now with the self-consistent TF calculation. We find that at densities $n_B$ of about 0.05 fm$^{-3}$ the cylindrical shape is very close to spherical nuclei and that at higher densities it almost merges with the solution corresponding to spherical nuclei. The difference between the slab shape and the other two shapes keeps on decreasing with increasing $n_B$. The spherical nucleus is the most favourable shape at all densities and at $n_B \sim 0.076$ fm$^{-3}$ all the three shapes are very close before melting into uniform npe matter. This value of the crust-core transition density is in harmony with the estimate of 0.072 fm$^{-3}$ obtained in the previous section using the CLDM with the same SLy4 interaction.

## 4 Crust-core phase transition and symmetry energy

The bottom of the inner crust is reached when a homogeneous phase, composed by neutrons, protons and electrons, which fill uniformly the whole WS cell, is energetically more favourable than any other possible pasta phase in the inner crust. As discussed before, to determine the crust-core transition from the crust

side is actually a delicate and time consuming task, as it can be seen from the reduced number of this type of calculations available in the literature [6, 12, 13, 18]. The study of the crust-core transition from the core side provides a simpler approach. To this end, we examine the stability conditions of the core under small-amplitude density fluctuations using the so-called thermodynamical [32–34] and dynamical [33, 35, 36] methods, using Skyrme forces.

In the thermodynamical method the stability is discussed in terms of the bulk properties of the EOS by imposing mechanical and chemical stability conditions

$$-\left(\frac{\partial P}{\partial v}\right)_{\mu_{np}} > 0 \qquad -\left(\frac{\partial \mu_{np}}{\partial q}\right)_{v} > 0, \tag{11}$$

where $P$ is the total pressure in $\beta$-stable matter, $\mu_{np} = \mu_n - \mu_p - \mu_e$, $v = 1/n_B$ is the volume and $q$ is the charge per baryon. From the solution of Eqs. (11) one obtains the crust-core transition density in the thermodynamical method [32–34, 37]. The dynamical method also includes effects from inhomogeneities of the density and from the Coulomb interaction. In this method one starts imposing small sinusoidal variations to the neutron, proton and electron densities, i.e.

$$\delta n_q(\mathbf{k}, \mathbf{r}) = \delta n_q(\mathbf{k}) e^{i\mathbf{kr}}, \tag{12}$$

where $q \in npe$ and $n_q(\mathbf{k})$ is the density in momentum space which fulfills $n_q(\mathbf{k}) = n_q^*(-\mathbf{k})$ to ensure that the variations of the particle are real. Next we expand the energy up to second order in the variation of the densities:

$$E = E_0 + \frac{1}{2}\sum_{i,j}\int d\mathbf{k} \frac{\delta^2 E}{\delta n_i(\mathbf{k}) \delta n_j^*(\mathbf{k})}, \tag{13}$$

where $E_0$ is the energy in the uniform phase and the subindices $i, j$ concern the different type of particles. The second order variation of the energy in the integrand of Eq. (13) can be written in a matrix form, which is required to be convex in order to ensure the stability against simultaneous variations of the neutron, proton and electron densities [33, 34]. The solution of this stability condition allows to determine the crust-core transition density within the dynamical method.

In the two panels of Figure 3 we show the thermodynamical and dynamical estimates of the crust-core transition density and pressure as a function of the slope of the symmetry energy calculated with different Skyrme forces. We display by filled (open) symbols the transition densities computed using the thermodynamical (dynamical) method. From this Figure two comments are in order. First, the dynamical predictions of the crust-core transition density and pressure are always smaller than the thermodynamical values, owing to the inclusion of finite size effects. Second, both the transition density and pressure, estimated by both methods, show a downwards tendency with increasing values of the slope parameter $L$. This trend is much more linear for the transition densities than for

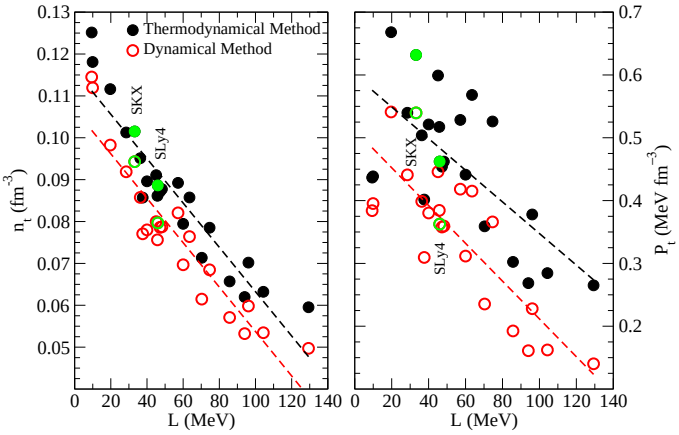


Figure 3. Core-crust transition density and pressure against the slope of the symmetry energy for several Skyrme forces, calculated using the thermodynamical method (black filled dots) and the dynamical method (red unfilled dots) in the core. The results of the interactions SkX ($L = 33.2$ MeV) and SLy4 ($L = 46$ MeV) discussed in the text are shown in green color.

the transition pressures [38]. Finally, we shall point out that in Section 2 we have estimated the crust-core transition density from the crust side using the CLDM with the SLy4 (0.072 fm$^{-3}$) and SkX (0.086 fm$^{-3}$) Skyrme forces. These values are about 10% smaller than the dynamical predictions, which are 0.080 and 0.094 fm$^{-3}$, respectively. These differences may be related to the method used to obtain the transition density. In this respect, the transition density calculated with SLy4 using the TF approach is $\sim 0.076$ fm$^{-3}$ (Section 3).

One also can obtain the mass-radius (M-R) relation of NS by integrating the Tolman-Oppenheimer-Volkov equations [1]. Recently, it has been shown that

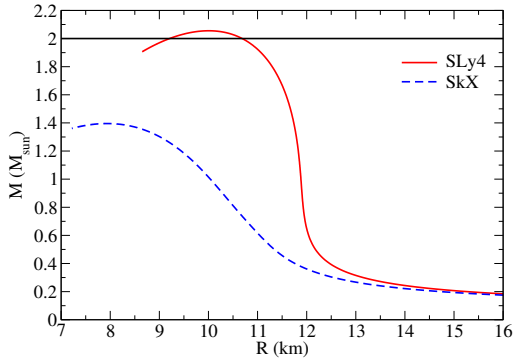


Figure 4. Mass-radius relation of neutron stars predicted by the SLy4 and SkX forces.

under a suitable thin crust approximation the M-R relation of the star can be predicted to good accuracy using the EOS of the core only [39]. In Figure 4 we show the M-R relation calculated with the SkX and SLy4 forces applying the method of Ref. [39]. We see that the maximum mass predicted by SLy4 is above two solar masses, as required by the astronomical observations, while the prediction of SkX is just about the standard value of a canonical neutron star of 1.4 solar masses. The fact that SLy4 predicts heavier stars that SkX may be related to the stiffer symmetry energy of SLy4 ($L = 46$ MeV) than SkX ($L = 33.2$ MeV), which leads to a stiffer neutron matter pressure in SLy4. As indicated by the results discussed in this section, the forces with stiffer symmetry energy (larger $L$) also use to have smaller values of the core-crust transition density and pressure.

## 5 Conclusions

We have analyzed the possible existence of a shape transition in the inner crust of neutron stars with the Compressible Liquid Drop Model and the self-consistent Thomas-Fermi approximation using Skyrme interactions. These semiclassical methods allow to study different shapes associated to spherical, cylindrical and planar geometries such as droplets, rods, slabs, tubes and bubbles in a rather simple way. The predictions from the Compressible Liquid Drop Model and the Thomas-Fermi model, in particular the transition densities from the crust to the core, are found to be in good agreement between them.

We have also computed the density and pressure corresponding to the crust-core transition proceeding from the core side using the thermodynamical and dynamical methods, which search the density value in homogeneous matter where the instabilities against formation of nuclear clusters appear. We find that the estimates of the transition density from the crust and core sides are in harmony between them. We have also examined the behaviour of the crust-core properties as a function of the slope of the symmetry energy. It is found that both, density and pressure, follow a downwards tendency with increasing values of the slope of the symmetry energy, with a fairly linear behaviour for the transition densities. Our study in this work points out the appearance of pasta phases in the inner crust for large values of the crust-core transition density and therefore for small values of the slope of the symmetry energy. Also, our results seem to suggest that the requirement of two solar masses for the maximum mass of neutron stars is more easily reached by Skyrme interactions with relatively small crust-core transition density and therefore that may not predict pasta phases in the inner crust.

## Acknowledgments

Work partially supported by Grants FIS2014-54672-P from MINECO, 2014SGR-401 from Generalitat de Catalunya and MDM-2014-0369 ICCUB (Unidad de Excelencia María de Maeztu) from MINECO. C.G. also acknowledges Grant BES-2015-074210 from MINECO.

## References

[1] S.L. Shapiro and S.A. Teukolsky (1983) *Black holes, white dwarfs and neutron stars: The physics of compact objets* (Wiley-Interscience, New York).
[2] G. Baym, H.A. Bethe and C.J. Pethick (1971) *Nucl. Phys.* **A175**, 225.
[3] S.B. Rüster, M. Hempel and J. Schaffner-Bielich (2006) *Phys. Rev.* **C73** 035804.
[4] X. Roca-Maza and J. Piekarewicz (2008) *Phys. Rev.* **C78** 025807.
[5] J.M. Pearson, S. Goriely and N. Chamel (2011) *Phys. Rev.* **C83** 065810.
[6] B.K. Sharma, M. Centelles, X. Viñas, M. Baldo and G.F. Burgio (2015) *Astron. Astrophys.* **584**, A103.
[7] J.W. Negele and D. Vautherin (1973) *Nucl. Phys.* **A207** 298.
[8] P.M. Pizzochero, F. Barranco, E. Vigezzi and R.A. Broglia (2002) *Astrophys. J.* **569** 381.
[9] M. Baldo, E.E. Saperstein and S.V. Tolokonnikov (2007) *Eur. Phys. J.* **A32** 97.
[10] F. Grill, J. Margueron and N. Sandulescu (2011) *Phys. Rev.* **C84** 065801.
[11] A. Pastore, S. Baroni and C. Losa (2011) *Phys. Rev.* **C84** 065807.
[12] J.M. Lattimer and D.F. Swesty (1991) *Nucl. Phys.* **A535**, 331.
[13] F. Douchin and P. Haensel (2001) *Astron. Astrophys.* **380**, 151.
[14] K. Oyamatsu (1993) *Nucl. Phys.* **A561**, 431
[15] M. Onsi, A.K. Dutta, H. Chatri et al (2008) *Phys. Rev.* **C77** 065805.
[16] J.M. Pearson, N. Chamel, S. Goriely and C. Ducoin (2012) *Phys. Rev.* **C85** 065803.
[17] K.S. Cheng, C.C. Yao and Z.G Dai (1997) *Phys. Rev.* **C55** 2092.
[18] H. Shen, H. Toki, K. Oyamatsu and K. Sumiyoshi (1998) *Nucl. Phys.* **A637** 435.
[19] S.S. Avancini, D.P. Menezes, M.D. Alloy et al (2008) *Phys. Rev.* **C78** 015802.
[20] F. Grill, C. Providência and S.S. Avancini (2012) *Phys. Rev.* **C85** 055808.
[21] X. Viñas, C. Gonzalez-Boquera, B.K. Sharma and M. Centelles (2017) *Acta Phys. Pol. Proc. Suppl.* **10** 259.
[22] J.M. Lattimer. C.J. Pethick, D.G. Ravenhall and R.Q. Lamb (1985) *Nucl. Phys.* **A432** 646.
[23] M. Centelles, M. Del Estal and X. Viñas (1998) *Nucl. Phys.* **A635** 193.
[24] M. Del Estal, M. Centelles and X. Viñas (1999) *Nucl. Phys.* **A 650** 443.
[25] F. Douchin, P. Haensel and J. Meyer (2000) *Nucl. Phys.* **A665** 419.
[26] M. Brack, C. Guet, H.-B. Håkanson (1985) *Phys. Rep.* **123** 275.
[27] T. Sil, J.N. De, S.K. Samaddar, et al. (2002) Phys. Rev. **C66**, 045803.
[28] M. Baldo et al., (2014) *Phys. of At. Nucl.* **77** 1157.
[29] M. Baldo, P. Schuck and X. Viñas (2008) *Phys. Lett.* **B663** 390.

[30] M. Baldo, L.M. Robledo, P. Schuck and X. Viñas (2013) *Phys. Rev.* **C84** 064305.
[31] E. Chabanat et al., (1998) *Nucl. Phys.* **A635** 231.
[32] S. Kubis (2007) *Phys. Rev.* **C76** 025801.
[33] J. Xu, L.W. Chen, B.A. Li and H.R. Ma (2009) Astrophys. J. **697** 549.
[34] C. Gonzalez-Boquera, M. Centelles, X. Viñas, A. Rios (2017) arXiv:1706.02736.
[35] C.J. Pethick, D.G. Ravenhall and C.P. Lorentz (1995) *Nucl. Phys.* **A584** 675.
[36] C. Ducoin, Ph. Chomaz and F. Gulminelli (2007) *Nucl. Phys.* **A789** 403.
[37] T.R. Routray et al., (2016) J. of Phys. **G43** 105101.
[38] A. Sulaksono, N. Alam and B.K. Agrawal, (2014) *Int. J. Mod. Phys. E* **23** 1450072.
[39] J.L. Zdunik, M. Fortin and P. Haensel (2017) *Astron. Astrophys.* **599** A119.